Letter

T2K measurements of muon neutrino and antineutrino disappearance using 3.13×10^{21} protons on target

K. Abe,[53] N. Akhlaq,[44] R. Akutsu,[27] A. Ali,[31] C. Alt,[10] C. Andreopoulos,[51,33] M. Antonova,[18] S. Aoki,[30] T. Arihara,[56] Y. Asada,[65] Y. Ashida,[31] E. T. Atkin,[20] Y. Awataguchi,[56] G. J. Barker,[62] G. Barr,[41] D. Barrow,[41] M. Batkiewicz-Kwasniak,[14] A. Beloshapkin,[25] F. Bench,[33] V. Berardi,[21] L. Berns,[55] S. Bhadra,[66] A. Blondel,[50,12] S. Bolognesi,[5] T. Bonus,[64] B. Bourguille,[17] S. B. Boyd,[62] A. Bravar,[12] D. Bravo Berguño,[1] C. Bronner,[53] S. Bron,[12] A. Bubak,[49] M. Buizza Avanzini,[9] S. Cao,[15] S. L. Cartwright,[48] M. G. Catanesi,[21] A. Cervera,[18] D. Cherdack,[16] G. Christodoulou,[11] M. Cicerchia,[23,*] J. Coleman,[33] G. Collazuol,[23] L. Cook,[41,27] D. Coplowe,[41] A. Cudd,[6] G. De Rosa,[22] T. Dealtry,[32] C. C. Delogu,[23] S. R. Dennis,[33] C. Densham,[51] A. Dergacheva,[25] F. Di Lodovico,[29] S. Dolan,[11] T. A. Doyle,[32] J. Dumarchez,[50] P. Dunne,[20] A. Eguchi,[52] L. Eklund,[13] S. Emery-Schrenk,[5] A. Ereditato,[2] A. J. Finch,[32] G. A. Fiorentini,[66] C. Francois,[2] M. Friend,[15,†] Y. Fujii,[15,†] R. Fukuda,[57] Y. Fukuda,[36] K. Fusshoeller,[10] C. Giganti,[50] M. Gonin,[9] A. Gorin,[25] M. Guigue,[50] D. R. Hadley,[62] P. Hamacher-Baumann,[47] M. Hartz,[59,27] T. Hasegawa,[15,†] S. Hassani,[5] N. C. Hastings,[15] Y. Hayato,[53,27] A. Hiramoto,[31] M. Hogan,[7] J. Holeczek,[49] N. T. Hong Van,[19,26] T. Honjo,[40] F. Iacob,[23] A. K. Ichikawa,[31] M. Ikeda,[53] T. Ishida,[15,†] M. Ishitsuka,[57] K. Iwamoto,[52] A. Izmaylov,[25] N. Izumi,[57] M. Jakkapu,[15] B. Jamieson,[63] S. J. Jenkins,[48] C. Jesús-Valls,[17] P. Jonsson,[20] C. K. Jung,[38,‡] P. B. Jurj,[20] M. Kabirnezhad,[41] H. Kakuno,[56] J. Kameda,[53] S. P. Kasetti,[34] Y. Kataoka,[53] Y. Katayama,[65] T. Katori,[29] E. Kearns,[3,27,‡] M. Khabibullin,[25] A. Khotjantsev,[25] T. Kikawa,[31] H. Kikutani,[52] S. King,[29] J. Kisiel,[49] T. Kobata,[40] T. Kobayashi,[15,†] L. Koch,[41] A. Konaka,[59] L. L. Kormos,[32] Y. Koshio,[39,‡] A. Kostin,[25] K. Kowalik,[37] Y. Kudenko,[25,§] S. Kuribayashi,[31] R. Kurjata,[61] T. Kutter,[34] M. Kuze,[55] L. Labarga,[1] J. Lagoda,[37] M. Lamoureux,[23] D. Last,[42] M. Laveder,[23] M. Lawe,[32] R. P. Litchfield,[13] S. L. Liu,[38] A. Longhin,[23] L. Ludovici,[24] X. Lu,[41] T. Lux,[17] L. N. Machado,[22] L. Magaletti,[21] K. Mahn,[35] M. Malek,[48] S. Manly,[45] L. Maret,[12] A. D. Marino,[6] L. Marti-Magro,[53,27] T. Maruyama,[15,*] T. Matsubara,[15] K. Matsushita,[52] C. Mauger,[42] K. Mavrokoridis,[33] E. Mazzucato,[5] N. McCauley,[33] J. McElwee,[48] K. S. McFarland,[45] C. McGrew,[38] A. Mefodiev,[25] M. Mezzetto,[23] A. Minamino,[65] O. Mineev,[25] S. Mine,[4] M. Miura,[53,‡] L. Molina Bueno,[10] S. Moriyama,[53,‡] Th. A. Mueller,[9] L. Munteanu,[5] Y. Nagai,[6] T. Nakadaira,[15,†] M. Nakahata,[53,27] Y. Nakajima,[53] A. Nakamura,[39] K. Nakamura,[27,15,†] Y. Nakano,[30] S. Nakayama,[53,27] T. Nakaya,[31,27] K. Nakayoshi,[15,†] C. E. R. Naseby,[20] T. V. Ngoc,[19,‖] V. Q. Nguyen,[50] K. Niewczas,[64] Y. Nishimura,[28] E. Noah,[12] T. S. Nonnenmacher,[20] F. Nova,[51] J. Nowak,[32] J. C. Nugent,[13] H. M. O'Keeffe,[32] L. O'Sullivan,[48] T. Odagawa,[31] T. Ogawa,[15] R. Okada,[39] K. Okumura,[54,27] T. Okusawa,[40] R. A. Owen,[44] Y. Oyama,[15,†] V. Palladino,[22] V. Paolone,[43] M. Pari,[23] W. C. Parker,[46] S. Parsa,[12] J. Pasternak,[20] M. Pavin,[59] D. Payne,[33] G. C. Penn,[33] L. Pickering,[35] C. Pidcott,[48] G. Pintaudi,[65] C. Pistillo,[2] B. Popov,[50,¶] K. Porwit,[49] M. Posiadala-Zezula,[60] A. Pritchard,[33] B. Quilain,[9] T. Radermacher,[47] E. Radicioni,[21] B. Radics,[10] P. N. Ratoff,[32] C. Riccio,[38] E. Rondio,[37] S. Roth,[47] A. Rubbia,[10] A. C. Ruggeri,[22] C. Ruggles,[13] A. Rychter,[61] K. Sakashita,[15,†] F. Sánchez,[12] G. Santucci,[66] C. M. Schloesser,[10] K. Scholberg,[8,‡] M. Scott,[20] Y. Seiya,[40,**] T. Sekiguchi,[15,†] H. Sekiya,[53,27,‡] D. Sgalaberna,[10] A. Shaikhiev,[25] A. Shaykina,[25] M. Shiozawa,[53,27] W. Shorrock,[20] A. Shvartsman,[25] K. Skwarczynski,[37] M. Smy,[4] J. T. Sobczyk,[64] H. Sobel,[4,27] F. J. P. Soler,[13] Y. Sonoda,[53] R. Spina,[21] S. Suvorov,[25,50] A. Suzuki,[30] S. Y. Suzuki,[15,†] Y. Suzuki,[27] A. A. Sztuc,[20] M. Tada,[15,†] M. Tajima,[31] A. Takeda,[53] Y. Takeuchi,[30,27] H. K. Tanaka,[53,‡] Y. Tanihara,[65] M. Tani,[31] N. Teshima,[40] L. F. Thompson,[48] W. Toki,[7] C. Touramanis,[33] T. Towstego,[58] K. M. Tsui,[33] T. Tsukamoto,[15,†] M. Tzanov,[34] Y. Uchida,[20] M. Vagins,[27,4] S. Valder,[62] D. Vargas,[17] G. Vasseur,[5] C. Vilela,[11] W. G. S. Vinning,[62] T. Vladisavljevic,[51] T. Wachala,[14] J. Walker,[63] J. G. Walsh,[32] Y. Wang,[38] D. Wark,[51,41] M. O. Wascko,[20] A. Weber,[51,41] R. Wendell,[31,‡] M. J. Wilking,[38] C. Wilkinson,[2] J. R. Wilson,[29] K. Wood,[38] C. Wret,[45] J. Xia,[54] K. Yamamoto,[40,**] C. Yanagisawa,[38,††] G. Yang,[38] T. Yano,[53] K. Yasutome,[31] N. Yershov,[25] M. Yokoyama,[52,‡] T. Yoshida,[55] M. Yu,[66] A. Zalewska,[14] J. Zalipska,[37] K. Zaremba,[61] G. Zarnecki,[37] M. Ziembicki,[61] M. Zito,[50] and S. Zsoldos[29]

(The T2K Collaboration)

[1]*University Autonoma Madrid, Department of Theoretical Physics, 28049 Madrid, Spain*
[2]*University of Bern, Albert Einstein Center for Fundamental Physics, Laboratory for High Energy Physics (LHEP), Bern, Switzerland*
[3]*Boston University, Department of Physics, Boston, Massachusetts, USA*
[4]*University of California, Irvine, Department of Physics and Astronomy, Irvine, California, USA*
[5]*IRFU, CEA, Université Paris-Saclay, F-91191 Gif-sur-Yvette, France*
[6]*University of Colorado at Boulder, Department of Physics, Boulder, Colorado, USA*
[7]*Colorado State University, Department of Physics, Fort Collins, Colorado, USA*
[8]*Duke University, Department of Physics, Durham, North Carolina, USA*

[9]*Ecole Polytechnique, IN2P3-CNRS, Laboratoire Leprince-Ringuet, Palaiseau, France*
[10]*ETH Zurich, Institute for Particle Physics and Astrophysics, Zurich, Switzerland*
[11]*CERN European Organization for Nuclear Research, CH-1211 Genve 23, Switzerland*
[12]*University of Geneva, Section de Physique, DPNC, Geneva, Switzerland*
[13]*University of Glasgow, School of Physics and Astronomy, Glasgow, United Kingdom*
[14]*H. Niewodniczanski Institute of Nuclear Physics PAN, Krakow, Poland*
[15]*High Energy Accelerator Research Organization (KEK), Tsukuba, Ibaraki, Japan*
[16]*University of Houston, Department of Physics, Houston, Texas, USA*
[17]*Institut de Fisica d'Altes Energies (IFAE), The Barcelona Institute of Science and Technology, Campus UAB, Bellaterra (Barcelona) Spain*
[18]*IFIC (CSIC & University of Valencia), Valencia, Spain*
[19]*Institute For Interdisciplinary Research in Science and Education (IFIRSE), ICISE, Quy Nhon, Vietnam*
[20]*Imperial College London, Department of Physics, London, United Kingdom*
[21]*INFN Sezione di Bari and Università e Politecnico di Bari, Dipartimento Interuniversitario di Fisica, Bari, Italy*
[22]*INFN Sezione di Napoli and Università di Napoli, Dipartimento di Fisica, Napoli, Italy*
[23]*INFN Sezione di Padova and Università di Padova, Dipartimento di Fisica, Padova, Italy*
[24]*INFN Sezione di Roma and Università di Roma "La Sapienza," Roma, Italy*
[25]*Institute for Nuclear Research of the Russian Academy of Sciences, Moscow, Russia*
[26]*International Centre of Physics, Institute of Physics (IOP), Vietnam Academy of Science and Technology (VAST), 10 Dao Tan, Ba Dinh, Hanoi, Vietnam*
[27]*Kavli Institute for the Physics and Mathematics of the Universe (WPI), The University of Tokyo Institutes for Advanced Study, University of Tokyo, Kashiwa, Chiba, Japan*
[28]*Keio University, Department of Physics, Kanagawa, Japan*
[29]*King's College London, Department of Physics, Strand, London WC2R 2LS, United Kingdom*
[30]*Kobe University, Kobe, Japan*
[31]*Kyoto University, Department of Physics, Kyoto, Japan*
[32]*Lancaster University, Physics Department, Lancaster, United Kingdom*
[33]*University of Liverpool, Department of Physics, Liverpool, United Kingdom*
[34]*Louisiana State University, Department of Physics and Astronomy, Baton Rouge, Louisiana, USA*
[35]*Michigan State University, Department of Physics and Astronomy, East Lansing, Michigan, USA*
[36]*Miyagi University of Education, Department of Physics, Sendai, Japan*
[37]*National Centre for Nuclear Research, Warsaw, Poland*
[38]*State University of New York at Stony Brook, Department of Physics and Astronomy, Stony Brook, New York, USA*
[39]*Okayama University, Department of Physics, Okayama, Japan*
[40]*Osaka City University, Department of Physics, Osaka, Japan*
[41]*Oxford University, Department of Physics, Oxford, United Kingdom*
[42]*University of Pennsylvania, Department of Physics and Astronomy, Philadelphia, Pennsylvania, 19104, USA*
[43]*University of Pittsburgh, Department of Physics and Astronomy, Pittsburgh, Pennsylvania, USA*
[44]*Queen Mary University of London, School of Physics and Astronomy, London, United Kingdom*
[45]*University of Rochester, Department of Physics and Astronomy, Rochester, New York, USA*
[46]*Royal Holloway University of London, Department of Physics, Egham, Surrey, United Kingdom*
[47]*RWTH Aachen University, III. Physikalisches Institut, Aachen, Germany*
[48]*University of Sheffield, Department of Physics and Astronomy, Sheffield, United Kingdom*
[49]*University of Silesia, Institute of Physics, Katowice, Poland*
[50]*Sorbonne Université, Université Paris Diderot, CNRS/IN2P3, Laboratoire de Physique Nucléaire et de Hautes Energies (LPNHE), Paris, France*
[51]*STFC, Rutherford Appleton Laboratory, Harwell Oxford, and Daresbury Laboratory, Warrington, United Kingdom*
[52]*University of Tokyo, Department of Physics, Tokyo, Japan*
[53]*University of Tokyo, Institute for Cosmic Ray Research, Kamioka Observatory, Kamioka, Japan*
[54]*University of Tokyo, Institute for Cosmic Ray Research, Research Center for Cosmic Neutrinos, Kashiwa, Japan*
[55]*Tokyo Institute of Technology, Department of Physics, Tokyo, Japan*
[56]*Tokyo Metropolitan University, Department of Physics, Tokyo, Japan*
[57]*Tokyo University of Science, Faculty of Science and Technology, Department of Physics, Noda, Chiba, Japan*
[58]*University of Toronto, Department of Physics, Toronto, Ontario, Canada*

[59]TRIUMF, Vancouver, British Columbia, Canada
[60]University of Warsaw, Faculty of Physics, Warsaw, Poland
[61]Warsaw University of Technology, Institute of Radioelectronics and Multimedia Technology, Warsaw, Poland
[62]University of Warwick, Department of Physics, Coventry, United Kingdom
[63]University of Winnipeg, Department of Physics, Winnipeg, Manitoba, Canada
[64]Wroclaw University, Faculty of Physics and Astronomy, Wroclaw, Poland
[65]Yokohama National University, Department of Physics, Yokohama, Japan
[66]York University, Department of Physics and Astronomy, Toronto, Ontario, Canada

(Received 25 August 2020; accepted 15 December 2020; published 26 January 2021)

We report measurements by the T2K experiment of the parameters θ_{23} and Δm^2_{32}, which govern the disappearance of muon neutrinos and antineutrinos in the three-flavor PMNS neutrino oscillation model at T2K's neutrino energy and propagation distance. Utilizing the ability of the experiment to run with either a mainly neutrino or a mainly antineutrino beam, muon-like events from each beam mode are used to measure these parameters separately for neutrino and antineutrino oscillations. Data taken from 1.49×10^{21} protons on target (POT) in neutrino mode and 1.64×10^{21} POT in antineutrino mode are used. The best-fit values obtained by T2K were $\sin^2(\theta_{23}) = 0.51^{+0.06}_{-0.07}(0.43^{+0.21}_{-0.05})$ and $\Delta m^2_{32} = 2.47^{+0.08}_{-0.09}(2.50^{+0.18}_{-0.13}) \times 10^{-3}\ \mathrm{eV}^2/c^4$ for neutrinos (antineutrinos). No significant differences between the values of the parameters describing the disappearance of muon neutrinos and antineutrinos were observed. An analysis using an effective two-flavor neutrino oscillation model where the sine of the mixing angle is allowed to take nonphysical values larger than 1 is also performed to check the consistency of our data with the three-flavor model. Our data were found to be consistent with a physical value for the mixing angle.

DOI: 10.1103/PhysRevD.103.L011101

I. INTRODUCTION

We present an update of T2K's ν_μ and $\bar{\nu}_\mu$ disappearance measurement from Ref. [1] with a larger statistical sample and significant analysis improvements. Data taken up until the end of 2018 are used. This is a beam exposure of 1.49×10^{21} (1.64×10^{21}) protons on target in neutrino (antineutrino) mode, an increase by a factor of 2.0 (2.2) over the previous result. While the same data were used for the result reported in Ref. [2], the result reported here focuses on events containing ν_μ and $\bar{\nu}_\mu$ candidates. These events are used to search for potential differences between neutrinos and antineutrinos and to test consistency with the PMNS oscillation model, by adding additional degrees of freedom to the oscillation probability formulas in the present analysis. These additional degrees of freedom are more straightforward to implement and interpret when studying muon-like events only.

The mixing of the three flavors of neutrinos without sterile neutrinos or nonstandard interactions is usually described with the PMNS formalism [3,4]. In this formalism, the vacuum oscillation probability is determined by six parameters: three angles (θ_{12}, θ_{13}, and θ_{23}), two mass-squared splittings (Δm^2_{21} and Δm^2_{32}, where $\Delta m^2_{ij} = m^2_i - m^2_j$), and a complex phase ($\delta_{CP}$). It is not known whether the smaller of the two mass splittings is between the two lightest states or the two heaviest states. These two cases are called normal and inverted ordering, respectively. ν_μ disappearance is not sensitive to this ordering, so all results here assume the normal mass ordering.

In this model, which assumes CPT conservation, ν_μ and $\bar{\nu}_\mu$ have identical survival probabilities for vacuum oscillations. At T2K's beam energy and baseline, the effect of the neutrinos propagating through matter on the muon neutrino survival probability is very small. Therefore, if the oscillation probabilities for neutrinos and antineutrinos differ by significantly more than expected, this could be interpreted as possible CPT violation and/or nonstandard interactions [5,6].

[*]also at INFN-Laboratori Nazionali di Legnaro
[†]Also at J-PARC, Tokai, Japan.
[‡]Affiliated member at Kavli IPMU (WPI), the University of Tokyo, Japan.
[§]Also at National Research Nuclear University "MEPhI" and Moscow Institute of Physics and Technology, Moscow, Russia.
[‖]Also at the Graduate University of Science and Technology, Vietnam Academy of Science and Technology.
[¶]Also at JINR, Dubna, Russia.
[**]Also at Nambu Yoichiro Institute of Theoretical and Experimental Physics (NITEP).
[††]Also at BMCC/CUNY, Science Department, New York, New York, USA.

In the three-flavor analysis shown here, the oscillation probabilities for ν_μ and $\bar{\nu}_\mu$ are calculated using the standard PMNS formalism, but with independent parameters to describe $\bar{\nu}_\mu$ and ν_μ oscillations, i.e., $\bar{\theta}_{23} \neq \theta_{23}$ and $\overline{\Delta m^2}_{32} \neq \Delta m^2_{32}$, where the barred parameters affect the antineutrino probabilities. As this dataset does not constrain the other PMNS parameters, they are assumed to be the same for ν and $\bar{\nu}$.

While it allows the ν_μ and $\bar{\nu}_\mu$ parameters to take different values, this three-flavor analysis does not allow oscillation probability values not allowed by the PMNS formalism. To test consistency with the PMNS formalism, we also present an analysis in which the oscillation probability is allowed to exceed the maximum possible PMNS value. In this analysis, for computational simplicity we approximate the probability for muon neutrino disappearance using a “two-flavor”-only oscillation formula with an effective mixing angle and mass splitting that takes into account the information we know about “three-flavor” mixing. $\sin^2(2\theta)$ is then allowed to take values exceeding 1, where θ is the effective neutrino mixing angle in this framework. This two-flavor approximation gives probabilities that agree within better than 0.5% with the full PMNS calculation across T2K’s neutrino energy range at the best-fit parameter values from T2K’s joint muon and electron-like event analysis [2].

II. EXPERIMENTAL APPARATUS

T2K [7] searches for neutrino oscillations in a long-baseline (295 km) neutrino beam sent from the Japan Proton Accelerator Research Complex (J-PARC) in Tokai, Japan to the Super-Kamiokande (SK) detector. SK [8,9] is situated 2.5° off the axis of the beam, meaning that it is exposed to a relatively narrow-energy-width neutrino flux, peaked around the oscillation maximum 0.6 GeV.

The neutrino beam generation starts with 30 GeV protons which strike a graphite target, producing hadrons, which are charge-selected and focused by three magnetic horns [10], and decay in a 96-m decay volume producing predominantly muon neutrinos. Positively or negatively charged hadrons are selected using the polarity of the horns, creating a beam dominated by neutrinos or antineutrinos, respectively.

A set of near detectors measures the unoscillated neutrino beam 280 m downstream of the interaction target. The INGRID [11] detector is an array of iron/scintillator sandwiches arranged in a cross pattern centered on the beam axis. INGRID measures the neutrino beam direction, stability, and profile [12].

The off-axis ND280 detector has three magnetized time projection chamber (TPC) trackers [13] and two fine-grained detectors (FGD1, made of CH, and FGD2, made of 52% water 48% CH by mass) [14], surrounded by an electromagnetic calorimeter [15]. A muon range detector [16] is located inside the magnet yokes. The magnetized tracker measures the momentum and charge of particles. ND280 constrains the ν_μ and $\bar{\nu}_\mu$ flux, the intrinsic ν_e and $\bar{\nu}_e$ contamination of the beam, and the interaction cross sections of different neutrino reactions.

The far detector, SK [8,9] is a 50 kt water Cherenkov detector, equipped with 11 129 inward-facing 20-inch photomultiplier tubes (PMTs) that image neutrino interactions in the pure water of the inner detector. SK also has 1885 outward-facing 8-inch PMTs instrumenting the outer detector, used to veto events with interaction vertices outside the inner detector.

III. ANALYSIS DESCRIPTION

The analysis presented here follows the same strategy as T2K’s PMNS three-flavor joint fit to muon disappearance and electron appearance data in Ref. [2]. A model is constructed that gives predictions of the spectra at the near and far detectors. This model uses simulations of the neutrino flux, interaction cross sections, and detector response and has variable parameters to account for both systematic and oscillation parameters. First, a fit of this model is performed to the near-detector data to tune and constrain the neutrino flux and interaction cross-section uncertainties. The results of this fit are then propagated to the far detector as a multivariate normal distribution described by a covariance matrix and the best-fit values for each systematic parameter. The far-detector data are then fit to constrain the oscillation parameters. This section describes each part of the analysis, focusing on changes from the analysis reported in Ref. [1]. Where not stated, the same procedure as in Ref. [2] is used. Particularly, the beam flux prediction, neutrino interaction modeling, systematic uncertainties, and near-detector event selection are unchanged, and the far-detector event selection used in this result is a subset of that in Ref. [2].

A. Beam flux prediction

The T2K neutrino flux and energy spectrum prediction is discussed extensively in Ref. [17]. The modeling of hadronic interactions is constrained by thin target hadron production data, from the NA61/SHINE experiment at CERN [18–22]. Before the ND280 analysis, the systematic uncertainties on the expected number of muon-like events after oscillations at SK due to the beam flux model are 8% and 7.3% for the ν_μ and $\bar{\nu}_\mu$ beams, respectively.

B. Neutrino interaction models

The ν_μ and $\bar{\nu}_\mu$ oscillation probabilities are expected to be symmetric, but their interaction probabilities with matter are not. For example, the interaction cross section for a charged-current quasielastic (CCQE) ν_μ interaction on oxygen is about 4 times higher than that for $\bar{\nu}_\mu$.

We model neutrino interactions using the NEUT interaction generator [23]. The interaction cross-section model and uncertainties used in this result are the same as in Ref. [2]. This model is significantly improved compared to the previous version of this analysis [1]. The treatment of multinucleon so-called 2p2h interactions [24,25] has been updated, with new uncertainties accounting for different rates of this interaction for neutrinos and antineutrinos, and for carbon and oxygen targets. We also allow the shape of the interaction cross section for 2p2h in energy-momentum transfer space to vary between that expected for a fully Δ-exchange-type interaction and that expected for a fully non-Δ-exchange-like interaction.

An uncertainty on the shielding of nucleons by the nucleus in CCQE interactions, modeled using the Nieves random phase approximation (RPA) method, has been added to the analysis [26–29]. The analysis also now accounts for mismodeling that could take place due to choosing an incorrect value for the nucleon removal energy in the CCQE process. Finally, a fit to external data [30,31] is now used to constrain our uncertainties on resonant single-pion production.

C. Near-detector event selection

We define 14 samples of near-detector events, each targeting a particular part of our flux or cross-section model. All selected events must have a reconstructed charged muon present as the highest momentum track, as we are targeting charged-current (CC) neutrino interactions. In neutrino beam mode, the muon is required to be negatively charged to target neutrino interactions. The neutrino mode samples are separated by the number of pions reconstructed: 0 pions, 1 positively charged pion, and any other number of pions, giving samples enriched in CCQE, CC single pion, and CC deep inelastic scattering interactions, respectively.

In antineutrino beam mode, there is one set of samples for positively charged muons and one set for negatively charged muons, allowing a separate constraint of the neutrino and antineutrino composition of the beam. This is important in antineutrino mode, as the interaction cross section for neutrinos is larger than for antineutrinos. The antineutrino mode samples are separated by the number of reconstructed tracks matched between the TPC and FGD: 1 or more than 1, giving samples enriched in CCQE or CC non-QE interactions, respectively. In both beam modes, samples are further separated by which FGD their vertices are reconstructed in. As in Ref. [2], the near-detector dataset for antineutrino mode is 1.38 times larger than in Ref. [1], while the neutrino-mode dataset is the same size.

D. Far-detector event selection

The analyses presented here target muon-like events. SK is not able to distinguish neutrinos from antineutrinos at an event-by-event level, as it cannot reconstruct the charge of the resulting muons. Hence, we form separate samples of events from neutrino and antineutrino beam mode to separately measure ν_μ and $\bar{\nu}_\mu$ oscillations.

SK's vertex position, momentum, and particle identification (PID) are reconstructed from the Cherenkov rings produced by charged particles traversing the detector. PID is possible because muons scatter little due to their large mass and hence produce a clear ring pattern, while electrons produce electromagnetic showers resulting in Cherenkov rings with diffuse edges. The ring's opening angle also helps to distinguish between electrons and muons. The samples used here require exactly one muon-like Cherenkov ring and no other rings to be reconstructed and are referred to as $1\mathrm{R}\mu$.

T2K's reconstruction algorithm [32] fits the number of photons and timing information from each SK PMT, allowing better signal-background discrimination and a fiducial volume increase of $\sim$20% over the previous algorithm used in Ref. [1]. Both $1\mathrm{R}\mu$ samples use the same selection criteria as in Ref. [2]. Table I shows the number of events predicted and observed for both $1\mathrm{R}\mu$ samples.

E. Systematic uncertainties and oscillation analysis

Our model includes systematic uncertainties from the neutrino flux prediction, the neutrino interaction cross-section model, and detector effects. We constrain several of these uncertainties by fitting our model to ND280 near-detector data in bins of muon momentum and angle. This ND280 constrained model is then used as the prior in the fits to the far-detector data, where the SK muon-like samples are binned in the neutrino energy reconstructed using lepton momentum and angle assuming a CCQE interaction. Table II shows the total systematic error in each $1\mathrm{R}\mu$ sample and a breakdown of the contributions from each uncertainty source. The near-detector fit introduces large anticorrelations between the parameters modeling the flux and cross-section uncertainties, so Table II also lists the overall contribution to the uncertainty from the combination of flux and cross-section uncertainties.

The near-detector fit reduces the systematic error on the expected number of events in the neutrino (antineutrino) mode $1\mathrm{R}\mu$ sample from 15% (13%) to 5.5% (4.4%).

In the three-flavor analysis, oscillation probabilities for all events are calculated using the full PMNS formulas [33], with matter effects (crust density, $\rho = 2.6\ \mathrm{g/cm^3}$ [34]). We allow the values of θ_{23} and Δm^2_{32} used in the neutrino

TABLE I. Number of events predicted using the best-fit oscillation parameter values from a previous T2K analysis [30], and the number of data events collected for both $1\mathrm{R}\mu$ samples.

Sample	Prediction	Data
ν-mode $1\mathrm{R}\mu$	272.34	243
$\bar{\nu}$-mode $1\mathrm{R}\mu$	139.47	140

TABLE II. Systematic uncertainty on the number of events in each of the 1Rμ samples broken down by uncertainty source. Neutrino cross-section parameter uncertainties (denoted "xsec") are broken down by whether they are constrained by ND280 data or not. Uncertainties due to final state interactions (FSI) and secondary interactions (SI) are incorporated in the analysis by adding them to the SK detector effect uncertainty, so these are listed together.

Error source	1Rμ ν-mode	1Rμ $\bar{\nu}$-mode
Flux (constr. by ND280)	4.3%	4.1%
Xsec (constr. by ND280)	4.7%	4.0%
Xsec (all)	5.6%	4.4%
Flux + Xsec (constr. by ND280)	3.3%	2.9%
Flux + Xsec (all)	5.4%	3.2%
SK detector effects + FSI + SI	3.3%	2.9%
Total	5.5%	4.4%

oscillation probability calculation to vary independently from those used for the antineutrino oscillation probability, in order to search for differences between neutrino and antineutrino oscillations.

In the two-flavor analysis, we use a modified version of the canonical two-flavor oscillation formula [35], where the disappearance probability for ν_μ ($\bar{\nu}_\mu$) is given by

$$P_{\nu_\mu\to\nu_\mu}(P_{\bar{\nu}_\mu\to\bar{\nu}_\mu}) \approx 1-\alpha(\bar{\alpha})\sin^2\left(1.267\frac{\Delta m^2[\mathrm{eV}^2]L[\mathrm{km}]}{E[\mathrm{GeV}]}\right),$$

where α plays the role of the well-known effective two-flavor mixing angle, $\sin^2 2\theta$. α differs from $\sin^2 2\theta$ in that it is allowed to take values larger than 1. The effective two-flavor Δm^2 used here can be obtained from the three-flavor oscillation parameters using the following equation:

$$\Delta m^2 = \Delta m^2_{32} + \sin^2\theta_{12}\Delta m^2_{21} + \cos\delta_{CP}\sin\theta_{13}\sin 2\theta_{12}\tan\theta_{23}\Delta m^2_{21}.$$

We use independent oscillation parameters for neutrinos and antineutrinos, with α and Δm^2 affecting neutrinos, and $\bar{\alpha}$ and $\overline{\Delta m^2}$ affecting antineutrinos.

When $\alpha > 1.0$, the ν_μ ($\bar{\nu}_\mu$) survival probability is negative at some points in (Δm^2, E_ν) parameter space. When weighting our Monte Carlo to produce predicted spectra for these points of parameter space, this gives negative oscillation probability weights for some events. We allow these negative event weights, but we do not allow the total predicted number of events in any bin of our event samples to be negative, setting them instead to 10^{-6} where this occurs.

For both the two-flavor and three-flavor analyses, a joint maximum-likelihood fit to both 1Rμ samples is performed. The likelihood used is a marginal likelihood, where all parameters except the parameters of interest are marginalized over.

The priors for the nuisance parameters are taken from the uncertainty model after the fit to ND280 data. Uniform priors are used in δ_{CP}, Δm^2_{32}, and $\sin^2\theta_{23}$. θ_{12} and Δm^2_{12} are fixed at their values from Ref. [36], due to their negligible effect on the ν_μ survival probability. The prior on θ_{13} is taken from Ref. [36].

We build frequentist confidence intervals, assuming the critical values for $\Delta\chi^2$ from a standard χ^2 distribution. $\Delta\chi^2$ is defined as the difference between the minimum χ^2 and the value for a given point in parameter space.

IV. RESULTS AND DISCUSSION

The reconstructed energy spectra of the ν_μ and $\bar{\nu}_\mu$ events observed during neutrino and antineutrino running modes are shown in Fig. 1. All fits discussed below are to both 1Rμ samples unless stated otherwise.

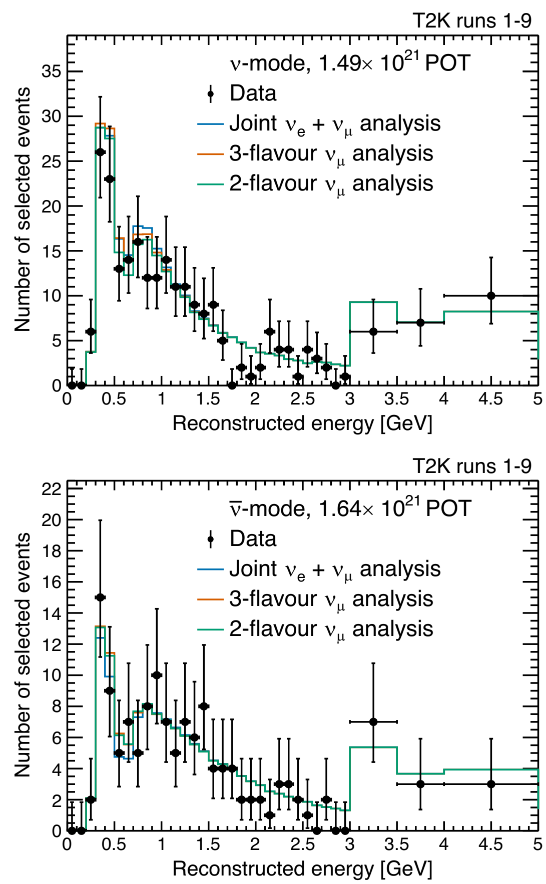

FIG. 1. Reconstructed energy spectra for the neutrino-mode (top) and antineutrino-mode (bottom) 1Rμ samples. The lines show the predicted number of events under several oscillation hypotheses: "Joint ν_e/ν_μ analysis" uses the best-fit values from a joint fit of the PMNS model to electron-like and muon-like data [2], "3-flavor ν_μ analysis" uses the best fit from the three-flavor fit reported here to the muon-like data, and "2-flavor ν_μ analysis" uses the best-fit value in the two-flavor fit reported here to the muon-like data. The uncertainty on the data includes all predicted event rates for which the measured number of data events is less than a Poisson standard deviation from that prediction.

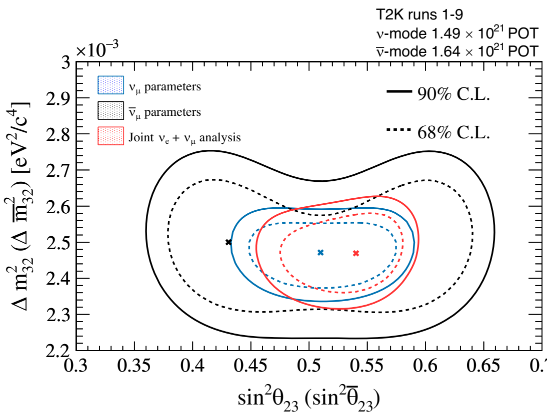

FIG. 2. 68% and 90% confidence intervals on $\sin^2\theta_{23}$ and Δm^2_{32} (blue) and $\sin^2\bar{\theta}_{23}$ and $\overline{\Delta m^2_{32}}$ (black) from the three-flavor analysis described here. Also shown are equivalent intervals on $\sin^2\theta_{23}$ and Δm^2_{32} (red) from a joint fit to muon-like and electron-like T2K data described in Ref. [2].

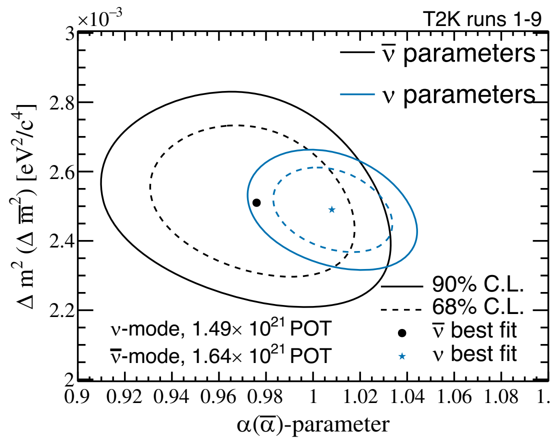

FIG. 3. 68% and 90% confidence intervals on the two-flavor analysis parameters affecting neutrinos (Δm^2, α) and antineutrinos ($\Delta\bar{m}^2$, $\bar{\alpha}$).

A. Three-flavor analysis

For normal ordering, the best-fit values obtained for the parameters describing neutrino oscillations are $\sin^2\theta_{23} = 0.51^{+0.06}_{-0.07}$ and $\Delta m^2_{32} = 2.47^{+0.08}_{-0.09} \times 10^{-3}$ eV$^2/c^4$, and those describing antineutrino oscillations are $\sin^2\bar{\theta}_{23} = 0.43^{+0.21}_{-0.05}$ and $\overline{\Delta m^2_{32}} = 2.50^{+0.18}_{-0.13} \times 10^{-3}$ eV$^2/c^4$. The best-fit value and uncertainty on $\overline{\Delta m^2_{32}}$ obtained for normal ordering are equivalent to those that would be obtained on $\overline{\Delta m^2_{31}}$ for inverted ordering.

Figure 2 shows the confidence intervals on the oscillation parameters applying to ν_μ overlaid on those for the parameters applying to $\bar{\nu}_\mu$. As the parameters for ν_μ and $\bar{\nu}_\mu$ show no significant incompatibility, this analysis provides no indication of new physics. We also show the confidence interval for Δm^2_{32} and $\sin^2\theta_{23}$ from the fit to electron-like and muon-like data in Ref. [2]. One can see by comparing these results that T2K's sensitivity to whether $\sin^2\theta_{23}$ is above or below 0.5 is driven by the electron-like samples, as the ν_μ disappearance probability depends at leading order on $\sin^2(2\theta_{23})$.

B. Two-flavor consistency check analysis

The best-fit values obtained on the effective two-flavor oscillation parameters are $\Delta m^2 = 2.49^{+0.08}_{-0.08}$ eV$^2/c^4$, $\alpha = 1.008^{+0.017}_{-0.016}$, $\overline{\Delta m^2} = 2.51^{+0.15}_{-0.14} \times 10^{-3}$ eV$^2/c^4$, $\bar{\alpha} = 0.976^{+0.029}_{-0.029}$. Fig. 3 shows the 68% and 90% confidence intervals for (Δm^2, α) and ($\overline{\Delta m^2}$, $\bar{\alpha}$). Both the 1σ confidence intervals include values of $\alpha(\bar{\alpha}) \leq 1.0$, indicating no significant disagreement between data and standard physical PMNS neutrino oscillations. We also see good compatibility between the parameters affecting neutrinos and antineutrinos.

C. Conclusions

We have shown separate measurements of the oscillation parameters governing ν_μ and $\bar{\nu}_\mu$ disappearance in long-baseline neutrino experiments using a significantly larger data sample and a much improved model of systematic uncertainties than those used in T2K's previous measurement of these parameters in Ref. [1]. We also show a consistency check between our data and the PMNS framework, where $\sin^2(2\theta)$ is allowed to take values larger than 1. In all analyses we find that the neutrino and antineutrino oscillation parameters are compatible with each other, and that our data are compatible with the PMNS framework. The results from these fits improve upon the sensitivity of and are not in significant disagreement with previous similar results from the MINOS Collaboration [37]. (Both show values of Δm^2_{32} around 2.5×10^{-3} eV$^2/c^4$ and θ_{23} consistent with maximal mixing.)

ACKNOWLEDGMENTS

We thank the J-PARC staff for superb accelerator performance. We thank the CERN NA61/SHINE Collaboration for providing valuable particle production data. We acknowledge the support of MEXT, Japan; NSERC (Grant No. SAPPJ-2014-00031), the NRC and CFI, Canada; the CEA and CNRS/IN2P3, France; the DFG, Germany; the INFN, Italy; the National Science Centre and Ministry of Science and Higher Education, Poland; the RSF (Grant No. 19-12-00325) and the Ministry of Science and Higher Education, Russia; MINECO and ERDF funds, Spain; the SNSF and State Secretary for Research and Innovation (SERI), Switzerland; the STFC, UK; and the DOE, USA. We also thank CERN for the UA1/NOMAD magnet, DESY for the HERA-B magnet mover system, NII for SINET5, the WestGrid and SciNet consortia in Compute Canada, and GridPP in the United

Kingdom. In addition, participation of individual researchers and institutions has been further supported by funds from the ERC (FP7), la Caixa Foundation (ID 100010434, fellowship code LCF/BQ/IN17/11620050), the European Unions Horizon 2020 Research and Innovation Programme under Marie Sklodowska-Curie Grant Agreement No. 713673 and No. 754496, and H2020 Grant No. RISE-GA822070-JENNIFER2 2020 and No. RISE-GA872549-SK2HK; the JSPS, Japan; the Royal Society, UK; French ANR Grant No. ANR-19-CE31-0001; and the DOE Early Career program, USA.

[1] K. Abe *et al.*, Updated T2K measurements of muon neutrino and antineutrino disappearance using 1.5e21 protons on target, Phys. Rev. D **96**, 011102 (2017).

[2] K. Abe *et al.*, Constraint on the matter-antimatter symmetry-violating phase in neutrino oscillations, Nature (London) **580**, 339 (2020).

[3] Z. Maki, M. Nakagawa, and S. Sakata, Remarks on the unified model of elementary particles, Prog. Theor. Phys. **28**, 870 (1962).

[4] B. Pontecorvo, Neutrino experiments and the problem of conservation of leptonic charge, Zh. Eksp. Teor. Fiz. **53**, 1717 (1967) [Sov. Phys. JETP **26**, 984 (1967)], http://www.jetp.ac.ru/cgi-bin/e/index/e/26/5/p984?a=list.

[5] V. A. Kostelecký and M. Mewes, Neutrinos with Lorentz-violating operators of arbitrary dimension, Phys. Rev. D **85**, 096005 (2012).

[6] O. G. Miranda and H. Nunokawa, Non standard neutrino interactions: Current status and future prospects, New J. Phys. **17**, 095002 (2015).

[7] K. Abe *et al.*, The T2K Experiment, Nucl. Instrum. Methods Phys. Res., Sect. A **659**, 106 (2011).

[8] Y. Fukuda *et al.*, The Super-Kamiokande detector, Nucl. Instrum. Methods Phys. Res., Sect. A **501**, 418 (2003).

[9] K. Abe *et al.*, Calibration of the Super-Kamiokande detector, Nucl. Instrum. Methods Phys. Res., Sect. A **737**, 253 (2014).

[10] T. Sekiguchi *et al.*, Development and operational experience of magnetic horn system for T2K experiment, Nucl. Instrum. Methods Phys. Res., Sect. A **789**, 57 (2015).

[11] M. Otani *et al.*, Design and construction of INGRID neutrino beam monitor for T2K neutrino experiment, Nucl. Instrum. Methods Phys. Res., Sect. A **623**, 368 (2010).

[12] K. Suzuki *et al.*, Measurement of the muon beam direction and muon flux for the T2K neutrino experiment, Prog. Theor. Exp. Phys. **2015**, 053C01 (2015).

[13] N. Abgrall *et al.*, Time projection chambers for the t2k near detectors, Nucl. Instrum. Methods **637**, 25 (2011).

[14] P.-A. Amaudruz *et al.*, The T2k fine-grained detectors, Nucl. Instrum. Methods **696**, 1 (2012).

[15] D. Allan *et al.*, The electromagnetic calorimeter for the T2K near detector ND280, J. Instrum. **8**, P10019 (2013).

[16] S. Aoki *et al.*, The T2K side muon range detector (SMRD), Nucl. Instrum. Methods Phys. Res., Sect. A **698**, 135 (2013).

[17] K. Abe *et al.*, T2K neutrino flux prediction, Phys. Rev. D **87**, 012001 (2013).

[18] N. Abgrall *et al.*, Measurements of cross sections and charged pion spectra in proton-carbon interactions at 31 GeV/c, Phys. Rev. C **84**, 034604 (2011).

[19] N. Abgrall *et al.*, Measurement of production properties of positively charged kaons in proton-carbon interactions at 31 GeV/c, Phys. Rev. C **85**, 035210 (2012).

[20] N. Abgrall *et al.*, Measurements of $\pi^{\pm}$, $K^{\pm}$, K_S^0, Λ and proton production in protoncarbon interactions at 31 GeV/c with the NA61/SHINE spectrometer at the CERN SPS, Eur. Phys. J. C **76**, 84 (2016).

[21] M. Posiadaa-Zezula, Recent T2K flux predictions with NA61/SHINE thin graphite target measurements, J. Phys. Conf. Ser. **888**, 012064 (2017).

[22] L. Zambelli, Hadroproduction experiments to constrain accelerator-based neutrino fluxes, J. Phys. Conf. Ser. **888**, 012021 (2017).

[23] Y. Hayato, A neutrino interaction simulation program library NEUT, Acta Phys. Pol. B **40**, 2477 (2009), https://www.actaphys.uj.edu.pl/R/40/9/2477/pdf.

[24] J. Nieves, I. R. Simo, and M. J. V. Vacas, Inclusive charged-current neutrino-nucleus reactions, Phys. Rev. C **83**, 045501 (2011).

[25] R. Gran, J. Nieves, F. Sanchez, and M. J. Vicente Vacas, Neutrino-nucleus quasi-elastic and 2p2h interactions up to 10 GeV, Phys. Rev. D **88**, 113007 (2013).

[26] J. Nieves, J. E. Amaro, and M. Valverde, Inclusive quasielastic charged-current neutrino-nucleus reactions, Phys. Rev. C **70**, 055503 (2004).

[27] J. Nieves, J. E. Amaro, and M. Valverde, Erratum: Inclusive quasielastic charged-current neutrino-nucleus reactions, Phys. Rev. C **70**, 055503 (2004); **72**, 019902 (2005).

[28] M. Valverde, J. E. Amaro, and J. Nieves, Theoretical uncertainties on quasielastic charged-current neutrino-nucleus cross sections, Phys. Lett. B **638**, 325 (2006).

[29] R. Gran, Model uncertainties for Valencia RPA effect for MINERνA, 2017.

[30] K. Abe *et al.*, Search for *CP* Violation in Neutrino and Antineutrino Oscillations by the T2K Experiment with 2.2×10^{21} Protons on Target, Phys. Rev. Lett. **121**, 171802 (2018).

[31] P. Stowell, C. Wret, C. Wilkinson, L. Pickering, S. Cartwright, Y. Hayato, K. Mahn, K. McFarland, J. Sobczyk, R. Terri, L. Thompson, M. Wascko, and Y. Uchida, NUISANCE: A neutrino cross-section generator tuning and comparison framework, J. Instrum. **12**, P01016 (2017).

[32] M. Jiang, K. Abe, C. Bronner, Y. Hayato, M. Ikeda, K. Iyogi, J. Kameda, Y. Kato, Y. Kishimoto, L. l. Marti *et al.*,

Atmospheric neutrino oscillation analysis with improved event reconstruction in Super-Kamiokande IV, Prog. Theor. Exp. Phys. **2019**, 053F01 (2019).

[33] V. D. Barger, K. Whisnant, S. Pakvasa, and R. J. N. Phillips, Matter effects on three-neutrino oscillations, Phys. Rev. D **22**, 2718 (1980).

[34] K. Hagiwara, N. Okamura, and K. Senda, The earth matter effects in neutrino oscillation experiments from Tokai to Kamioka and Korea, J. High Energy Phys. 09 (2011) 082.

[35] H. Nunokawa, S. J. Parke, and R. Zukanovich Funchal, Another possible way to determine the neutrino mass hierarchy, Phys. Rev. D **72**, 013009 (2005).

[36] M. Tanabashi *et al.*, Review of particle physics, Phys. Rev. D **98**, 030001 (2018).

[37] P. Adamson *et al.*, Combined Analysis of ν_μ Disappearance and $\nu_\mu \to \nu_e$ Appearance in MINOS Using Accelerator and Atmospheric Neutrinos, Phys. Rev. Lett. **112**, 191801 (2014).